Inflation from a no-scale supersymmetric $SU(4)_C \times SU(2)_L \times SU(2)_R$ model

Waqas Ahmed[1,*] and Athanasios Karozas[2,†]

[1]CAS Key Laboratory of Theoretical Physics, Institute of Theoretical Physics, Chinese Academy of Sciences, Beijing 100190, People's Republic of China

[2]Physics Department, Theory Division, Ioannina University, GR-45110 Ioannina, Greece

(Received 3 May 2018; published 25 July 2018)

We study inflation in a supersymmetric Pati-Salam model driven by a potential generated in the context of no-scale supergravity. The Pati-Salam gauge group $SU(4)_C \times SU(2)_L \times SU(2)_R$ is supplemented with a Z_2 symmetry. Spontaneous breaking via the $SU(4)$ adjoint leads to the left-right symmetric group. Then the $SU(2)_R$ breaks at an intermediate scale and the inflaton is a combination of the neutral components of the $SU(2)_R$ doublets. We discuss various limits of the parameter space, and we show that consistent solutions with the cosmological data for the spectral index n_s and the tensor-to-scalar ratio r are found for a wide range of the parameter space of the model. Regarding the latter, which is a canonical measure of primordial gravity waves, we find that $r \sim 10^{-3} - 10^{-2}$. An alternative possibility where the adjoint scalar field S has the rôle of the inflaton is also discussed.

DOI: 10.1103/PhysRevD.98.023538

I. INTRODUCTION

In cosmological models, inflation is realized by a slowly rolling scalar field, the so called inflaton, whose energy density dominates the early history Universe [1–4]. Among several suggestions regarding its origin, the economical scenario that this field can be identified with the Standard Model (SM) Higgs state h, has received considerable attention [5]. In this approach, the Higgs field drives inflation through its strong coupling, $\xi h^2 R$, where R is the Ricci scalar and ξ is a dimensionless parameter that acquires a large value, $\xi \gtrsim 10^4$.

In modern particle physics theories, cosmological inflation is usually described within the framework of supergravity or superstring grand unified theories (GUTs). In these theories, the SM is embedded in a higher gauge symmetry and the field content including the Higgses are incorporated in representations of the higher symmetry which includes the SM gauge group. In this context, several new facts and constraints should be taken into account. For instance, since new symmetry breaking stages are involved, the Higgs sector is usually extented and alternative possibilities for identifying the inflaton emerge. In addition, the effective potential has a specific structure constrained from fundamental principles of the theory. In string theory effective models, e.g., in a wide class of compactifications the scalar potential appears with a no-scale structure as in standard supergravity theories [6,7]. In general, the scalar potential is a function of the various fields which enter in a complicated manner through the superpotential W and the Kähler potential K. Thus, a rather detailed investigation is required to determine the conditions for slow roll inflation and ensure a stable inflationary trajectory in such models. Modifications of the basic no-scale Kähler potential and various choices for the superpotential have been studied leading to a number of different inflationary cases [8–14], while studies of inflation within supergravity in a model independent way can be found in [15,16].

In the present work, we implement the scenario of Higgs inflation in a model based on the Pati-Salam gauge symmetry $SU(4)_C \times SU(2)_L \times SU(2)_R$ [17] (denoted for brevity with 4-2-2). This model has well known attractive features (see e.g., the recent review [18]) and has been successfully rederived in superstring and D-brane theories [19–22]. Early universe cosmology and inflationary predictions of the model (or its extensions) have been discussed previously in several works [23–25]. Here we consider a supersymmetric version of the 4-2-2 model where the breaking down to the SM gauge group takes place in two steps. First $SU(4)$ breaks spontaneously at the usual supesymmetric GUT scale $M_{\rm GUT} \gtrsim 10^{16}$ GeV, down to the *left-right* group[1] via the adjoint representation. Then,

*waqasmit@itp.ac.cn
†akarozas@cc.uoi.gr

[1]For a recent discussion on left-right models based on GUTs, see [26]. Inflation from an $SO(10)$ model with left-right intermediate symmetry is analyzed in [27].

depending on the specific structure of the Higgs sector, the $SU(2)_R$ scale can break either at the GUT scale, i.e., simultaneously with $SU(4)$, or at some lower, intermediate energy scale. The variety of possibilities are reflected back to the effective field theory model implying various interesting phenomenological consequences. Regarding the Higgs inflation scenario, in particular, the inflaton field can be identified with the neutral components of the $SU(2)_R$ doublet fields associated with the intermediate scale symmetry breaking. In this work, we will explore alternative possibilities to realize inflation where the inflaton is identified with the $SU(2)_R$ doublets. We also examine the case of inflation in the presence of the adjoint representation.

The layout of the paper is as follows. In Sec. II, we present a brief description of the 4-2-2 model, focusing in its particle content and the symmetry breaking pattern. In Sec. III, we present the superpotential and the emergent no-scale supergavity Kähler potential of the effective model. We derive the effective potential and analyze the predictions on inflation when either the $SU(2)_R$ doublets or the adjoint play the rôle of the inflaton. We present our conclusions in Sec. IV.

II. DESCRIPTION OF THE MODEL

In this section, we highlight the basic ingredients of the model with gauge symmetry,

$$SU(4)_C \times SU(2)_L \times SU(2)_R. \tag{2.1}$$

This model unifies each family of quarks and leptons into two irreducible representations, F_i and $\bar{F}_i$ transforming as [28]

$$F_i = (4,2,1)_i \quad \text{and} \quad \bar{F}_i = (\bar{4},1,2)_i,$$

under the corresponding factors of the gauge group (2.1). Here the subscript i ($i = 1, 2, 3$) denotes family index. Note that $F + \bar{F}$ comprise the 16 of $SO(10)$, $16 \to (4,2,1) + (\bar{4},1,2)$. The explicit embedding of the SM matter fields, including the right-handed neutrino is as follows:

$$F_i = \begin{pmatrix} u_r & u_g & u_b & \nu \\ d_r & d_g & d_b & e \end{pmatrix}_i, \quad \bar{F}_i = \begin{pmatrix} u_r^c & u_g^c & u_b^c & \nu^c \\ d_r^c & d_g^c & d_b^c & e^c \end{pmatrix}_i, \tag{2.2}$$

where the subscript (r, g, b) are color indices.

The symmetry breaking

$$SU(4)_C \times SU(2)_R \to SU(3)_C \times U(1)_Y, \tag{2.3}$$

is achieved by introducing two Higgs multiplets

$$H = (\bar{4},1,2) = \begin{pmatrix} u_H^c & u_H^c & u_H^c & \nu_H^c \\ d_H^c & d_H^c & d_H^c & e_H^c \end{pmatrix},$$
$$\bar{H} = (4,1,2) = \begin{pmatrix} \bar{u}_H^c & \bar{u}_H^c & \bar{u}_H^c & \bar{\nu}_H^c \\ \bar{d}_H^c & \bar{d}_H^c & \bar{d}_H^c & \bar{e}_H^c \end{pmatrix} \tag{2.4}$$

which descend from the 16 and $\overline{16}$ of $SO(10)$, respectively.

An alternative way to break the gauge symmetry arises in the case where the adjoint scalar $\Sigma = (15,1,1)$ is included in the spectrum. We parametrize Σ with a singlet scalar field S

$$\Sigma \equiv (15,1,1) = \frac{S}{2\sqrt{3}} \begin{pmatrix} 1 & 0 & 0 & 0 \\ 0 & 1 & 0 & 0 \\ 0 & 0 & 1 & 0 \\ 0 & 0 & 0 & -3 \end{pmatrix}, \tag{2.5}$$

which acquires a GUT scale vacuum expectation value (vev) $\langle S \rangle \equiv v \simeq 3 \times 10^{16}$ GeV breaking $SU(4) \to SU(3) \times U(1)$. The breaking leads to the left-right symmetric group, $SU(3)_C \times SU(2)_L \times SU(2)_R \times U(1)_{B-L}$, and the decomposition of the Higgs fields H, $\bar{H}$ is as follows:

$$H(\bar{4},1,2) \to Q_H(\bar{3},1,2)_{-1/3} + L_H(1,1,2)_1$$
$$\bar{H}(4,1,2) \to \bar{Q}_H(3,1,2)_{1/3} + \bar{L}_H(1,1,2)_{-1} \tag{2.6}$$

where $Q_H = (u_H^c \; d_H^c)^T$, $\bar{Q}_H = (\bar{u}_H^c \; \bar{d}_H^c)$ and $L_H = (\nu_H^c \; e_H^c)^T$, $\bar{L}_H = (\bar{\nu}_H^c \; \bar{e}_H^c)$.

The right-handed doublets L_H, $\bar{L}_H$, acquiring vev's along their neutral components $\nu_H^c, \bar{\nu}_H^c$ and as a result they break the $SU(2)_R$ symmetry at some scale M_R. This way we obtain the symmetry breaking pattern [21]:

$$SU(4)_C \times SU(2)_R \times SU(2)_L$$
$$\to SU(3)_C \times U(1)_{B-L} \times SU(2)_R \times SU(2)_L$$
$$\to SU(3) \times SU(2)_L \times U(1)_Y.$$

The two scales $M_{\rm GUT}$ and M_R are not related to each other and it is, in principle, possible to take M_R at some lower scale provided there is no conflict with observational data such as flavor changing neutral currents and lepton or baryon number violation. Regarding the fast proton decay problem, in particular, in 4-2-2 models, due to absence of the associated gauge bosons there are no contributions from dimension six (d-6) operators, and related issues from d-5 operators can be remedied with appropriate symmetries in the superpotential.

The remaining spectrum and its $SO(10)$ origin is as follows: The decomposition of the 10 representation of $SO(10)$, gives a bidoublet and a sextet field, transforming under the 4-2-2 symmetry as follows

$$10 \to h(1,2,2) + D_6(6,1,1)\cdot \tag{2.7}$$

The two Higgs doublets of the minimal supersymmetric standard model (MSSM) descend from the bidoublet

$$h = (1,2,2) = \begin{pmatrix} h_2^+ & h_1^0 \\ h_2^0 & h_1^- \end{pmatrix}. \tag{2.8}$$

Also, the sextet of (2.7) decomposes into a pair of colored triplets: $D_6 \to D_3(3,1,1) + \bar{D}_3(\bar{3},1,1)$.

Collectively we have the following SM assignments:

$$\begin{aligned}
F &= (4,2,1) \to Q\left(3,2,\frac{1}{6}\right) + L\left(1,2,-\frac{1}{2}\right) \\
\bar{F} &= (\bar{4},1,2) \to u^c\left(\bar{3},1,-\frac{2}{3}\right) + d^c\left(\bar{3},1,\frac{1}{3}\right) \\
&\quad + e^c(1,1,1) + \nu^c(1,1,0) \\
h &= (1,2,2) \to H_u\left(1,2,\frac{1}{2}\right) + H_d\left(1,2,-\frac{1}{2}\right) \\
H &= (\bar{4},1,2) \to u_H^c\left(\bar{3},1,-\frac{2}{3}\right) + d_H^c\left(\bar{3},1,\frac{1}{3}\right) \\
&\quad + e_H^c(1,1,1) + \nu_H^c(1,1,0) \\
\bar{H} &= (4,1,2) \to \bar{u}_H^c\left(3,1,\frac{2}{3}\right) + \bar{d}_H^c\left(3,1,-\frac{1}{3}\right) \\
&\quad + \bar{e}_H^c(1,1,-1) + \bar{\nu}_H^c(1,1,0) \\
D_6 &= (6,1,1) \to D_3\left(3,1,-\frac{1}{3}\right) + \bar{D}_3\left(\bar{3},1,\frac{1}{3}\right)
\end{aligned} \tag{2.9}$$

Fermions receive Dirac type masses from a common tree-level invariant term, $F\bar{F}h$, while right-handed (RH) neutrinos receive heavy Majorana contributions from non-renormalizable terms, to be discussed in the next sections. In addition, the color triplets d_H^c and $\bar{d}_H^c$ are combined with the D_3 and $\bar{D}_3$ states via the trilinear operators $HHD_6 + \bar{H}\,\bar{H}\,D_6$ and get masses near the GUT scale.

After the short description of the basic features of the model, in the following sections, we investigate various inflationary scenarios in the context of no-scale supergravity, by applying the techniques presented in [29,30].

III. INFLATION IN NO-SCALE SUPERGRAVITY

In this section, we consider the 4-2-2 model as an effective string theory model and study the implications of Higgs inflation. The 'light' spectrum in these constructions contains the MSSM states in representations transforming nontrivially under the gauge group and a number of moduli fields associated with the particular compactification. We will focus on the superpotential and the Kähler potential which are essential for the study of inflation.

The superpotential is a holomorphic function of the fields. Ignoring Yukawa interaction terms, the most general superpotential up to dimension four which is relevant to our discussion is

$$\begin{aligned}
W = {} & M\bar{H}H + \mu\bar{h}h + m\,\mathrm{tr}(\Sigma)^2 + n\bar{H}\Sigma H + c\,\mathrm{tr}(\Sigma^3) \\
& - \alpha(\bar{H}H)^2 - \beta(\bar{h}h)^2 - \beta'(\bar{H}H)(\bar{h}h) \\
& - \kappa\,\mathrm{tr}(\Sigma^4) - \lambda\bar{H}\,\mathrm{tr}(\Sigma^2)H
\end{aligned} \tag{3.1}$$

where from now on we set the reduced Planck mass to unity, $M_{\rm Pl} = 1$. We focus on the dynamics of inflation during the first symmetry breaking stages at high energy scales. For this reason we ignore all the terms involving the bi-doubled since this state mostly contribute in low energies by ginving mass to the MSSM particles and do not play an important rôle during inflation. In addition, we impose a Z_2 symmetry, under which Σ is odd and all the other fields are even. As a result the trilinear terms $\bar{H}\Sigma H$ and $\mathrm{tr}(\Sigma^3)$ are eliminated from the superpotential in (3.1). The elimination of these trilinear terms of the superpotential is important, since if we use $\bar{H}\Sigma H$ and $\mathrm{tr}(\Sigma^3)$ instead of $\bar{H}\mathrm{tr}(\Sigma^2)H$ and $\mathrm{tr}(\Sigma^4)$, the shape of the resulting potential is not appropriate and it leads to inconsistent results with respect to the cosmological bounds while at the same time returns a low scale value for the parameter M in the superpotential, which usually expected to be close to the GUT scale. Then, using (2.5) and (2.6) the superpotential takes the following form:

$$\begin{aligned}
W \supset {} & \left(M - \frac{\tilde{\lambda}}{9}S^2\right)\bar{Q}_H Q_H + (M - \tilde{\lambda}S^2)\bar{L}_H L_H \\
& - \alpha(\bar{Q}_H Q_H + \bar{L}_H L_H)^2 + mS^2 - \tilde{\kappa}S^4
\end{aligned} \tag{3.2}$$

where $\tilde{\lambda} = \frac{3\lambda}{4}$ and $\tilde{\kappa} = \frac{7\kappa}{12}$. From the phenomenological point of view we expect $\langle S\rangle = v$ to be at the GUT scale. By assuming $v \simeq 3\times 10^{16}$ GeV and using the minimization condition $\partial W/\partial S = 0$, we estimate that $m \simeq 2\tilde{\kappa}v^2$ which, for $\tilde{\kappa} = 1/2$, gives $m \sim 10^{14}$ GeV.

In the two-step breaking pattern that we consider here, $\bar{L}_H$ and L_H must remain massless at this scale in order to break the $SU(2)_R$ symmetry at a lower scale. The $SU(2)_R$ breaking scale should not be much lower than the GUT scale in order to have a realistic heavy Majorana neutrino scenario. In addition, we have to ensure that the colored triplets $\bar{Q}_H$ and Q_H will be heavy. In order to keep the $\bar{L}_H$, L_H doublets at a lower scale, and at the same time the colored fields $\bar{Q}_H$ and Q_H to be heavy, we assume that $M \approx \tilde{\lambda}\langle S\rangle^2 = \tilde{\lambda}v^2$. In this case, $\bar{Q}_H$, Q_H acquire GUT scale masses $M_{Q_H} \approx \frac{8\tilde{\lambda}}{9}\langle S\rangle^2$.

During inflation the colored triplets $\bar{Q}_H$, Q_H and the charged components of the RH doublets, $\bar{L}_H$ and L_H, do not play an important rôle. The $SU(2)_R$ symmetry breaks

via the neutral components[2] $\bar{\nu}_H$ and ν_H. In terms of these states, the superpotential reads

$$W = \tilde{\lambda}(v^2 - S^2)\bar{\nu}_H\nu_H - \alpha(\bar{\nu}_H\nu_H)^2 + mS^2 - \tilde{\kappa}S^4, \quad (3.3)$$

where we have made use of the relation $M \simeq \tilde{\lambda}v^2$.

The Kähler potential has a no-scale structure and is a Hermitian function of the fields and their conjugates. For the present analysis, we will consider the dependence of the Higgs fields of the 4-2-2 gauge group and the 'volume' modulus T. Therefore, assuming the fields $\phi_i = (S, T, H, h)$ and their complex conjugates, we write

$$K = -3\log\left[T + T^* - \frac{1}{3}(HH^* + \bar{H}\bar{H}^* + \mathrm{tr}\,\Sigma^\dagger\Sigma) + \frac{\xi}{3}(H\bar{H} + H^*\bar{H}^*) + \frac{\zeta}{3}(hh^* + \bar{h}\bar{h}^*)\right] \quad (3.4)$$

where ξ is a dimensionless parameter. In the expression (3.4), we can ignore the last term which involves the bidoublet and in terms of ν_H, $\bar{\nu}_H$ and S, the Kähler potential reads:

$$K = -3\log\left[T + T^* - \frac{1}{3}(|\nu_H|^2 + |\bar{\nu}_H|^2 + S^2) + \frac{\xi}{3}(\bar{\nu}_H\nu_H + (\bar{\nu}_H)^*(\nu_H)^*)\right]. \quad (3.5)$$

In order to determine the effective potential, we define the function

$$G = K + \log|W|^2 \equiv K + \log W + \log W^*.$$

Then the effective potential is given by

$$V = e^G(G_iG^{-1}_{ij^*}G_{j^*} - 3) + V_D \quad (3.6)$$

where $G_i(G_{j^*})$ is the derivative with respect to the field $\phi_i(\phi^*_j)$ and the indices i, j run over the various fields. V_D stands for the D-term contribution.

Computing the derivatives and substituting in (3.6) the potential takes the form

$$V[\bar{\nu}_H, \nu_H, S] = \frac{9}{(-3 + \nu_H^2 + \bar{\nu}_H^2 + S^2 - 2\xi\bar{\nu}_H\nu_H)^2} \times [(\tilde{\lambda}v^2 - 2\alpha\nu_H\bar{\nu}_H)^2(\nu_H^2 + \bar{\nu}_H^2) - 8\tilde{\lambda}mS^2\bar{\nu}_H\nu_H - 2\tilde{\lambda}S^2(\tilde{\lambda}v^2 - 2\alpha\nu_H\bar{\nu}_H)(\nu_H^2 + \bar{\nu}_H^2) + 4\tilde{\lambda}^2S^2(\bar{\nu}_H\nu_H)^2 + 4m^2S^2 - 16\tilde{\kappa}S^4(m - \tilde{\lambda}\bar{\nu}_H\nu_H) + \tilde{\lambda}^2S^4(\nu_H^2 + \bar{\nu}_H^2) + 16\tilde{\kappa}^2S^6] \quad (3.7)$$

where we have ignored the D-term contribution and we have assumed that the value of the T modulus field is stabilized at $\langle T\rangle = \langle T^*\rangle = 1/2$, see [31,32]. Notice that in the absence of the Higgs contributions in the Kähler potential, the effective potential is exactly zero, $V = 0$ due to the well known property of the no-scale structure.

We are going now to investigate two different inflationary cases: firstly, along H-direction and secondly along S-direction.

A. Inflation along H-direction

We proceed by parametrizing the neutral components of the L_H and $\bar{L}_H$ fields as $\nu_H = \frac{1}{2}(X + Y)e^{i\theta}$ and $\bar{\nu}_H = \frac{1}{2}(X - Y)e^{i\varphi}$, respectively. These yield

$$X = |\nu_H| + |\bar{\nu}_H|, \qquad Y = |\nu_H| - |\bar{\nu}_H|. \quad (3.8)$$

Assuming $\theta = 0$ and $\varphi = 0$, along the D-flat direction, $Y = 0$, and the combination X is identified with the inflaton. The shape of the potential, as a function of the fields S and X, is presented in Fig. 1. In order to avoid singularities from the denominator, we have assume a condition which is described in the following.

The potential along the $S = 0$ direction is:

$$V(X) = \frac{\tilde{\lambda}^2v^4X^2\left(1 - \frac{\alpha X^2}{2\tilde{\lambda}v^2}\right)^2}{2\left(1 - \left(\frac{1-\xi}{6}\right)X^2\right)^2}. \quad (3.9)$$

The shape of the $V(X, S)$ scalar potential presented in Fig. 1 along with the inflaton trajectory description and the simplified form in (3.9) is similar with the one presented in [29,30]. As it is usually the case in no-scale supergravity, the effective potential displays a singularity when the denominator vanishes. The presence of these singularities lead to an exponentially steep potential which can cause violation of the basic slow-roll conditions (i.e., $\varepsilon \ll 1$, $|\eta| \ll 1$). Consequently, these singularities must be removed. In our specific model described by the potential 3.9)), we first notice that for the special value $\xi = 1$ the potential is free from singularities. For generic values of ξ however, i.e., $\xi \neq 1$, the potential displays a singularity for $X = \sqrt{\frac{6}{1-\xi}}$. In order to remove the zeros of the denominator in (3.9), we assume the following condition [29],

[2]Here and for the rest of the paper, for shorthand we remove the subscript "c" on the fields, i.e.: $\bar{\nu}^c_H$, $\nu^c_H \to \bar{\nu}_H, \nu_H$.

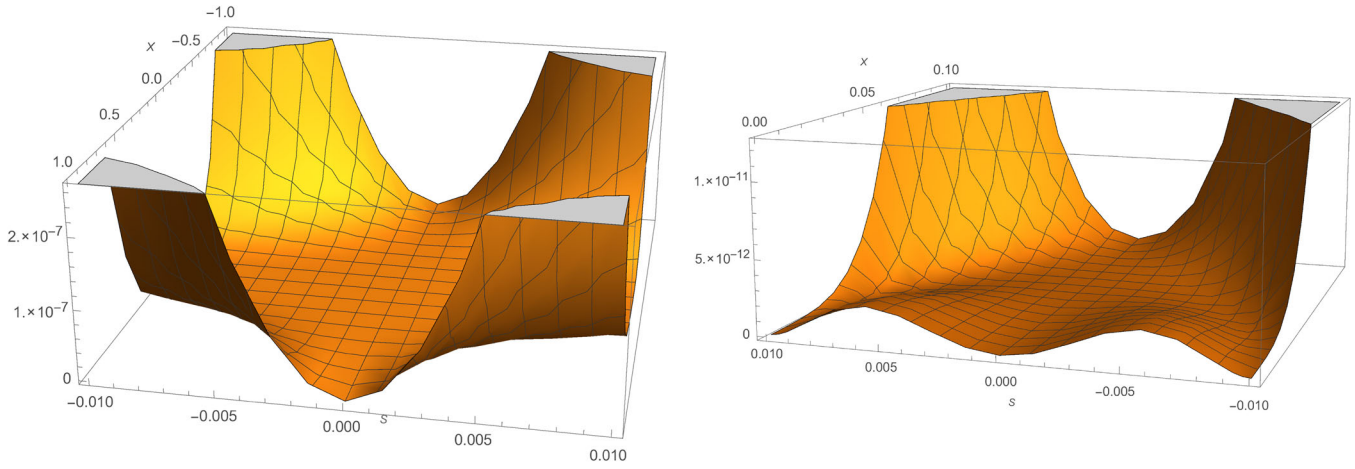

FIG. 1. Plots of the potential as a function of S and X and for appropriate values of the other parameters. The plot on the right displays a close-up view of the region with small values for X and S.

$$\alpha = \frac{(1-\xi)\tilde{\lambda}v^2}{3}. \tag{3.10}$$

This is a strong assumption which relates parameters with different origins. Indeed, α is a superpotential parameter while ξ descents from the Kahler potential. Since in our specific model the condition (3.10) lacks an explanation from first principles, it will be reasonable in the subsequent analysis to study the effects of a slightly relaxed version of (3.10). This can be achieved by introducing a small parameter δ (with $\delta \ll 1$) and modifying the condition as follows,

$$\alpha = \frac{(1-\xi+\delta)\tilde{\lambda}v^2}{3}. \tag{3.11}$$

In the remainder of this section, we are going to study the potential for special ξ values using the conditions (3.10) and (3.11).

We will start by analyzing some special cases first. By imposing (3.10), which means $\delta = 0$ the scalar potential simplifies to a quadratic monomial,

$$V(X) = \frac{\tilde{\lambda}^2 v^4}{2} X^2 \tag{3.12}$$

something that can be also seen from the plots in Fig. 1, where for small values of S (along the $S = 0$ direction) the potential receives a quadratic shape form. The Eq. (3.12) shows the potential of a chaotic inflation scenario. However, at this stage, the inflaton field X is not canonically normalized since its kinetic energy terms take the following form

$$\mathcal{L}(X) = \frac{1-\frac{\xi}{6}(1-\xi)X^2}{2(1-\frac{1}{6}(1-\xi)X^2)^2}(\partial X)^2 - \frac{\tilde{\lambda}^2 v^4}{2} X^2. \tag{3.13}$$

We introduce a canonically normalized field χ satisfying

$$\left(\frac{d\chi}{dX}\right)^2 = \frac{1-\frac{\xi}{6}(1-\xi)X^2}{(1-\frac{1}{6}(1-\xi)X^2)^2}. \tag{3.14}$$

After integrating, we obtain the canonically normalized field χ as a function of X

$$\chi = \sqrt{6}\tanh^{-1}\left(\frac{(1-\xi)X}{\sqrt{6\left(1-\frac{\xi(1-\xi)X^2}{6}\right)}}\right) - \sqrt{\frac{6\xi}{1-\xi}}\sin^{-1}\left(\sqrt{\xi\left(\frac{1-\xi}{6}\right)}X\right). \tag{3.15}$$

Next, we investigate the implications of Eq. (3.15) by considering two different cases, for $\xi = 0$ and $\xi \neq 0$.

(i) For $\xi = 0$ we have $X = \sqrt{6}\tanh(\frac{\chi}{\sqrt{6}})$ and the potential becomes,

$$V = 3\tilde{\lambda}^2 v^4 \tanh^2\left(\frac{\chi}{\sqrt{6}}\right), \tag{3.16}$$

which is analogous to the conformal chaotic inflation model (or T-Model) [33]. In these particular type of models, the potential has the general form

$$V(\chi) = \lambda^n \tanh^{2n}\left(\frac{\chi}{\sqrt{6}}\right) \quad \text{where} \quad n = 1, 2, 3, \ldots \tag{3.17}$$

As we can see, for $n = 1$ we receive our result in (3.16) with $\lambda = 3\tilde{\lambda}^2 v^4$. This potential can be further reduced to subcases depending upon the value of χ. For $\chi \geq 1$ the potential in Eq. (3.16) reduces to Starobinsky model [34]. In this case, the inflationary observables have values $(n_s, r) \approx (0.967, 0.003)$ and

the tree level prediction for $\xi = 0$ is consistent with the latest Planck bounds [35]. This type of models will be further analyzed in the next section where inflation along the S-direction is discussed.

(ii) The particular case of $\xi = 1$ implies a quadratic chaotic inflation and the tree-level inflationary prediction $(n_s, r) \approx (0.967, 0.130)$ is ruled out according to the latest *Planck* 2015 results. For $0 < \xi < 1$, the prediction for (n_s, r), can be worked out numerically.

After this analysis, we turn our attention to a numerical calculation. In our numerical analysis, we imply the modified condition (3.11) were as mentioned previously a small varying parameter δ has been introduced in order to soften the strict assumption (3.10). By substitute the relaxed condition (3.11) in (3.9) and neglecting $\mathcal{O}(\delta^2)$, the potential receives the following form:

$$V(X) \simeq \frac{\tilde{\lambda}^2 v^4}{2} X^2 \left(1 - \frac{2\delta X^2}{6 + (\xi - 1)X^2}\right). \tag{3.18}$$

As we observe the first term in the above relation is the quadratic potential (3.12), while the second term encodes the effects of the small parameter δ. In addition, we note that the order of the singularity enhancement have been improved in comparison with the initial potential (3.9). Next we present our numerical results where the rôle of the parameter δ is also discussed.

B. Numerical analysis

Before presenting numerical predictions of the model it is useful to briefly review here the basic results of the slow roll assumption. The inflationary slow roll parameters are given by [36,37]:

$$\epsilon = \frac{1}{2}\left(\frac{V'(X)}{V(X)\chi'(X)}\right)^2,$$
$$\eta = \left(\frac{V''(X)}{V(X)(\chi'(X))^2} - \frac{V'(X)\chi''(X)}{V(X)(\chi'(X))^3}\right). \tag{3.19}$$

The third slow-roll parameter is,

$$\varsigma^2 = \left(\frac{V'(X)}{V(X)\chi'(X)}\right)\left(\frac{V'''(X)}{V(X)(\chi'(X))^3} - 3\frac{V''(X)\chi''(X)}{V(X)(\chi'(X))^4} + 3\frac{V'(X)(\chi''(X))^2}{V(X)(\chi'(X))^5} - \frac{V'(X)\chi'''(X)}{V(X)(\chi'(X))^4}\right) \tag{3.20}$$

where a prime denotes a derivative with respect to X. The slow-roll approximation is valid as long as the conditions $\epsilon \ll 1, |\eta| \ll 1$ and $\varsigma^2 \ll 1$ hold true. In this scenario, the tensor-to-scalar ratio r, the scalar spectral index n_s and the running of the spectral index $\frac{dn_s}{d\ln k}$ are given by

$$r \simeq 16\epsilon, \quad n_s \simeq 1 + 2\eta - 6\epsilon, \quad \frac{dn_s}{d\ln k} \simeq 16\epsilon\eta - 24\epsilon^2 + 2\varsigma^2. \tag{3.21}$$

The number of e-folds is given by

$$N_l = \int_{X_e}^{X_l} \left(\frac{V(X)\chi'(X)}{V'(X)}\right) dX, \tag{3.22}$$

where l is the comoving scale after crossing the horizon, X_l is the field value at the comoving scale and X_e is the field when inflation ends, i.e., $\max(\epsilon(X_e), \eta(X_e), \varsigma(X_e)) = 1$. Finally, the amplitude of the curvature perturbation Δ_R is given by:

$$\Delta_R^2 = \frac{V(X)}{24\pi^2\epsilon(X)}. \tag{3.23}$$

Focusing now on the numerical analysis, we see that we have to deal with three parameters: ξ, δ and $\tilde{\lambda}$. We took the number of e-folds (N) to be 60, and in Fig. 2, we present two different cases in the $n_s - r$ plane, along with the Planck measurements (*Planck* TT,TE,EE+lowP) [35]. Specifically, in Fig. 1(a), we fixed ξ and vary $\tilde{\lambda}$ and δ. The various colored (dashed) lines corresponds to different fixed ξ-values. The green line corresponds to the limiting case with $\xi = 1$ and as we observe the results are more consistent with the Plank bounds (black solid contours) as the value of ξ decreases. Similar, in Fig. 1(b) we treat δ as a fixed parameter while we vary ξ and $\tilde{\lambda}$. Also, in this case, we observe that for a significant region of the parameter space the solutions are in good agreement with the observed cosmological bounds. The green curve here corresponds to $\delta = 10^{-6}$. The special case with $\delta = 10^{-6} \sim 0$ and $\xi = 1$ is represented by the black dot and as we discussed earlier is ruled out from the recent cosmological bounds. We observe from the plot that, as ξ approaches to unity the splitting between the curves due to different values of δ is small and the solution converges to $\delta \sim 0$ case. However, as we decrease the values of ξ we have splitting of the curves and better agreement with the cosmological bounds. Finally, in plots 1(c) and 1(d), we present values of the running of the spectral index with respect to n_s. We observe that the running of the spectral index, approximately receives values in the range $-5 \times 10^{-4} < \frac{dn_s}{d\ln k} < 5 \times 10^{-4}$.

Next we present additional plots to better clarify the rôle of the various parameters involved in the analysis.

Firstly, we study the spectral index n_s as a function of the various parameters. The results are presented in Fig. 3. In plots (a) and (b), we consider the cases with fixed values for ξ and δ, respectively, and we take variations for $\tilde{\lambda}$. We vary the parameter ξ in the range $\xi \sim [0.92, 1]$ with the most preferable solutions for $\xi \simeq [0.96, 1]$. In addition, the two plots suggest that acceptable solutions are found in the

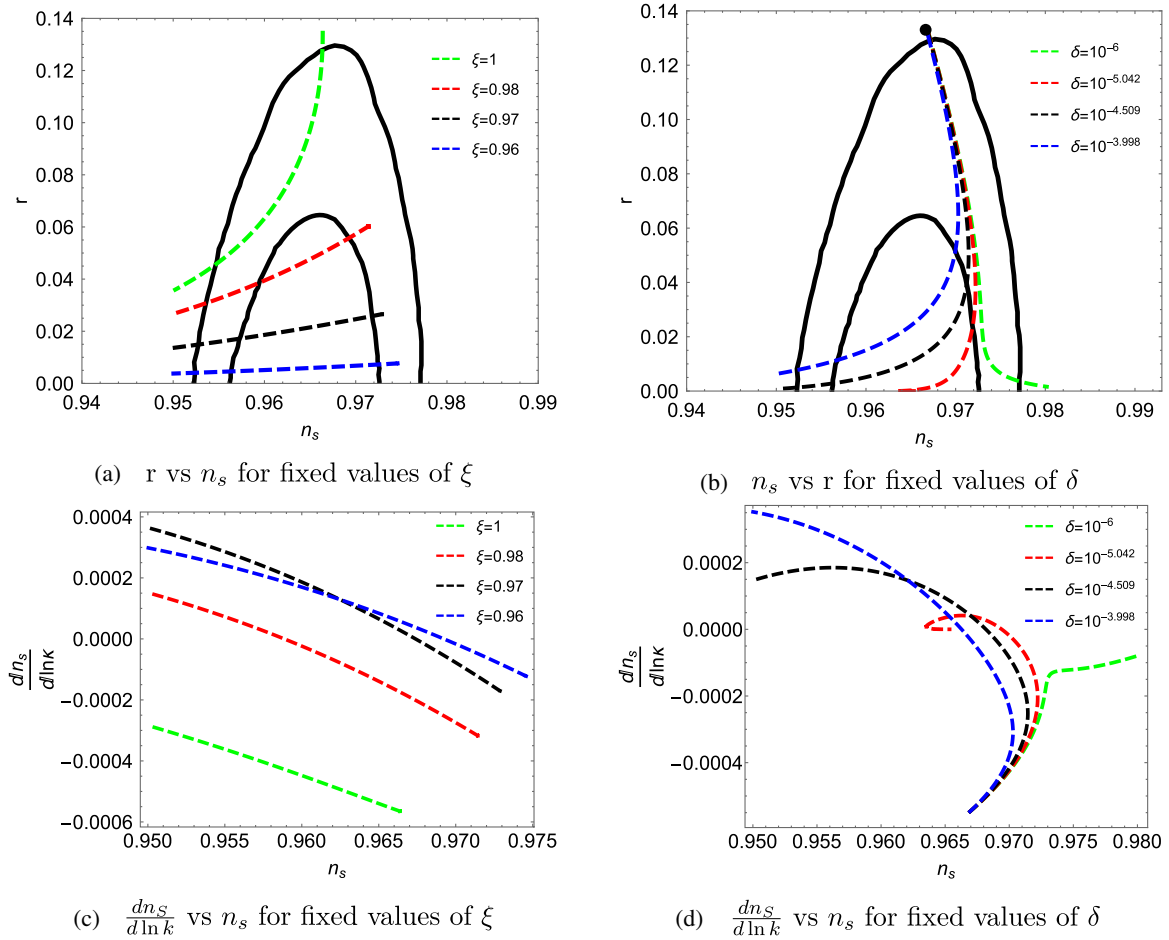

(a) r vs n_s for fixed values of ξ

(b) n_s vs r for fixed values of δ

(c) $\frac{dn_S}{d\ln k}$ vs n_s for fixed values of ξ

(d) $\frac{dn_S}{d\ln k}$ vs n_s for fixed values of δ

FIG. 2. The inflationary predictions (r-n_s) and ($\frac{dn_s}{d\ln k} - n_s$) of the model by varying the various parameters involved in to the analysis. In all cases, we took the number of e-folds, $N = 60$. In plots (a) and (b), black solid contours represents the Planck constraints (*Planck* TT,TE,EE+lowP) at 68% (inner) and 95% (outer) confidence level [35]. In plots (a) and (c), we keep ξ constant for each curve and vary $\tilde{\lambda}$ and δ. While in plots (b) and (d) for each curve we fixed δ and vary $\tilde{\lambda}$ and ξ. The black dot solution corresponds to $\xi = 1$.

range $\tilde{\lambda} \sim [10^{-2}, 10^{-1}]$. In plots (c) and (d), n_s is depicted in terms of δ and ξ, respectively. As we expected, the dependence on δ is negligible when it receives very small values, since we observe from plot 3(c) that the various curves are almost constant for very small δ values. The results are become more sensitive on δ as we decrease the value of ξ. This behavior can also be confirmed from the potential (3.18). As we can see for $\xi \sim 1$ the second term is simplified and the potential receives a chaotic like form. In this case, the effects of small δ in the observables are almost negligible (green line). However as we decrease the value of ξ and we increase the values of δ the second term becomes important and contributes to the results.

Next, in Fig. 4 we consider various cases for the tensor to scalar ratio, r. The description of the plots follows the spirit of those presented in Fig. 3 for the spectral index n_S. In particular, by comparing the plots 4(c) and 3(c) we notice that the dependence of r on δ is weaker in comparison with n_S. Thus the relaxation parameter δ strongly affects the spectral index n_S while for $\delta < 10^{-4}$ and fixed ξ the tensor-scalar ratio r remains almost constant. In summary, from the various figures presented so far we observe that consistent solutions can be found in a wide range of the parameter space. We also note that the model predicts solutions with $r \leq 0.02$, which is a prediction that can be tested with the discovery of primordial gravity waves and with bounds of future experiments.

Regarding the superpotential parameter $\tilde{\lambda}$, we can see from the various plots that its value must be within the range $\tilde{\lambda} \sim [10^{-2}, 10^{-1}]$. Using this range of values for $\tilde{\lambda}$ and the fact that, $M_{Q_H} \approx \frac{8\tilde{\lambda}}{9} v^2$, with $v \simeq 10^{-2}$ in $M_{\rm Pl} = 1$ units we conclude that: $M_{Q_H} \sim [0.217, 2.17] \times 10^{13}$ GeV. The fact that the mass value is small compare to the $\mathcal{O}(M_{\rm GUT})$ scale, can create tension with other phenomenological predictions of the model, like unification of gauge couplings. On the other hand, as already mentioned, Q_H, $\bar{Q}_H$ triplet fields can be mixed with the triplets D_3, $\bar{D}_3$ contained in the sextet D_6, something that is possible to lead in a significant lift to the mass value of the extra triplet fields.

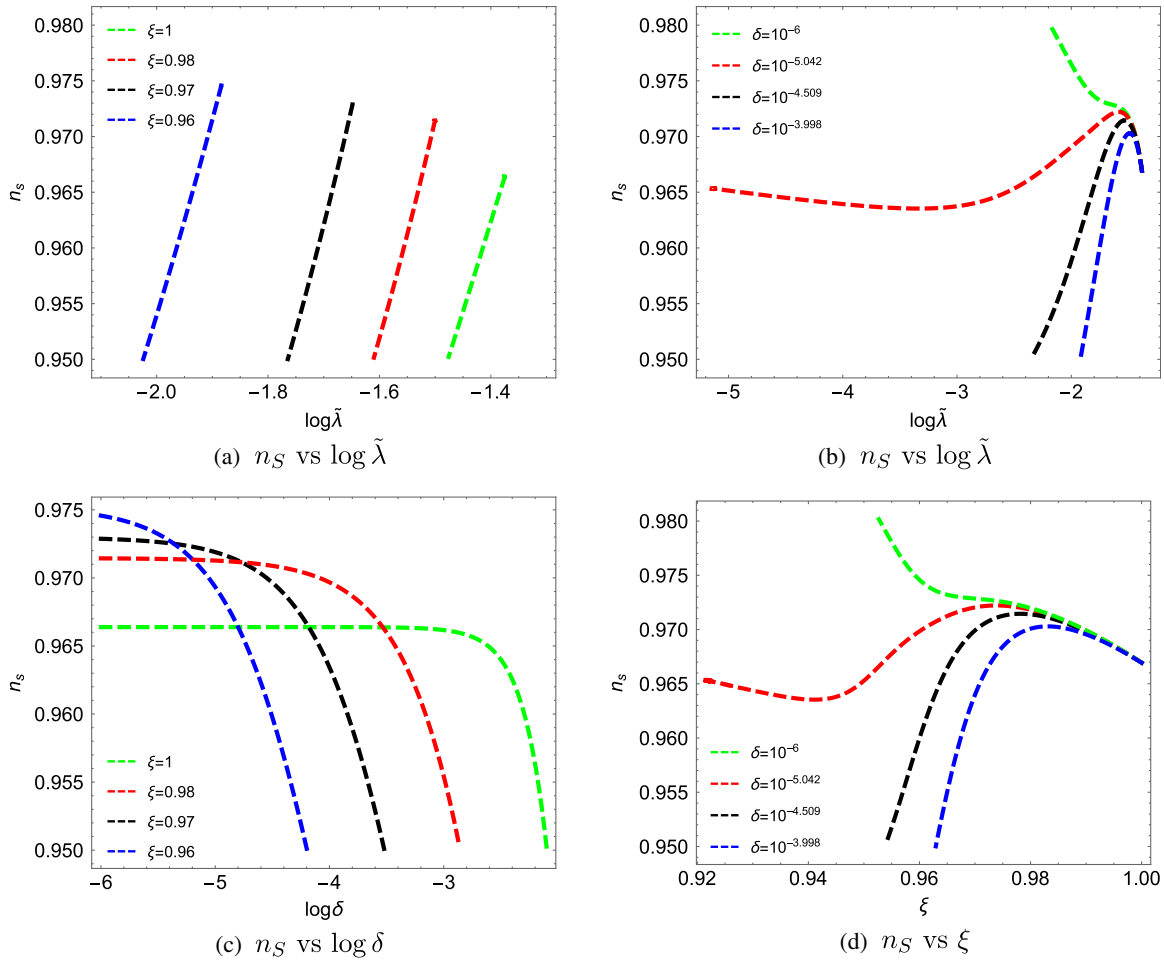

(a) n_S vs $\log\tilde{\lambda}$ (b) n_S vs $\log\tilde{\lambda}$

(c) n_S vs $\log\delta$ (d) n_S vs ξ

FIG. 3. Plots (a) and (c) show how n_S depends on $\log\tilde{\lambda}$ and $\log\delta$, respectively. For each curve in plots (a),(c), we fixed the value of ξ and vary $\tilde{\lambda}$ and δ. Similarly, plots (b) and (d), shows n_s vs $\log(\tilde{\lambda})$ and n_S vs ξ, respectively. In plots (b) and (d), the value of δ is fixed while we vary the other parameters.

It is also interesting to investigate the values of the Hubble parameter during inflation $H_{\rm inf}$ in the model. In the slow-roll limit, the Hubble parameter it depends on the value of X:

$$H_{\rm inf}^2 = \frac{V(X)}{3M_{\rm Pl}^2} \tag{3.24}$$

and we evaluate it at the pivot scale. In Fig. 5, we show the values of the Hubble parameter in the $(H_{\rm inf} - n_s)$ plane. We observe that the values of the Hubble parameter with respect to n_s bounds are of order 10^{13} GeV.

C. Reheating

As has already been discussed in Sec. II, the quarks and leptons in the 4-2-2 model are unified under the representations $F_i = (4, 2, 1)$ and $\bar{F}_i = (\bar{4}, 1, 2)$, where $i = 1, 2, 3$ denote the families and the RH-neutrinos are contained in the $\bar{F}$ representation. A heavy Majorana mass for the RH-neutrinos can be realized from the following non-renormalizable term,

$$M_{\nu^c}\nu^c\nu^c \approx \gamma\frac{\bar{F}\,\bar{F}\,\bar{H}\,\bar{H}}{M_*}, \tag{3.25}$$

where we have suppressed generation indices for simplicity, γ is a coupling constant and M_* represents a high cut-off scale (e.g., the compactification scale in a string model or the Planck scale $M_{\rm Pl}$). In terms of $SO(10)$ GUTs, this operator descent from the following invariant operator

$$16_F 16_F \bar{16}_H \bar{16}_H$$

and as described in [38] can be used to explain the reheating process of the universe after the end of inflation. In our case, the 4-2-2 symmetry breaking occur in two steps: first $G_{PS} \xrightarrow{\langle S\rangle} G_{L-R}$ and then $G_{L-R} \xrightarrow{\langle\nu_H\rangle,\langle\bar{\nu}_H\rangle} G_{\rm SM}$. The first breaking is achieved via the adjoint of the PS group at the GUT scale while the second breaking occurs in an intermediate scale M_R. After the breaking of the L-R symmetry, the high order term in (3.25) gives the following Majorana mass term for the RH neutrinos

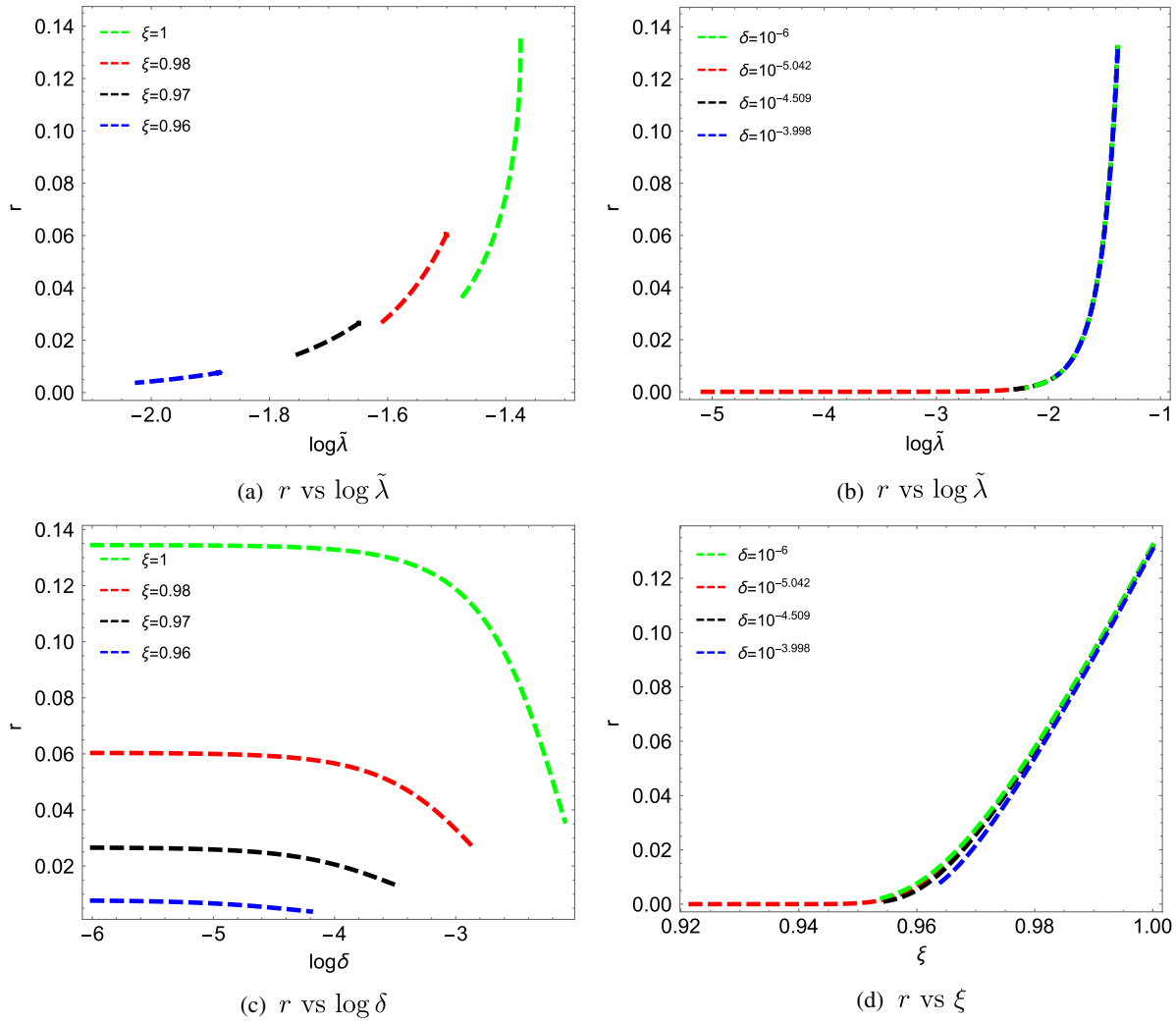

(a) r vs $\log\tilde{\lambda}$ (b) r vs $\log\tilde{\lambda}$

(c) r vs $\log\delta$ (d) r vs ξ

FIG. 4. Plots (a) and (c) show r vs $\log\tilde{\lambda}$ and r vs $\log\delta$, respectively. For each curve in plots (a) and (c), we fixed ξ and vary $\tilde{\lambda}$ and δ. Similar, in plots (b) and (d), we present r vs $\log\tilde{\lambda}$ and r vs ξ. For each curve in these plots we fixed the value of δ and vary $\tilde{\lambda}$ and ξ.

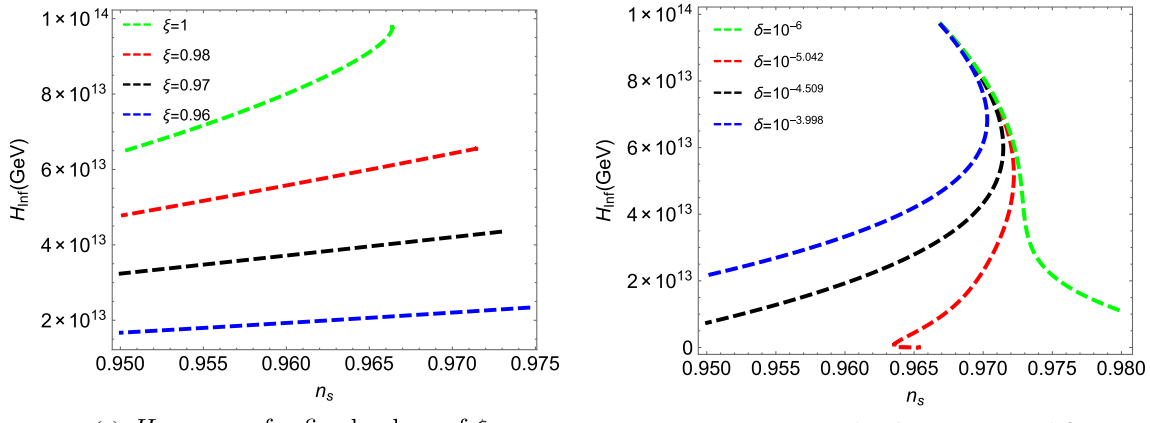

(a) H_{inf} vs n_s for fixed values of ξ (b) H_{inf} vs n_s for fixed values of δ

FIG. 5. Plots showing the values (in GeV) of the Hubble parameter with respect to the scalar spectral index n_s. For acceptable n_s values we see that the Hubble parameter receives values of order $10^{13} - 10^{14}$ GeV.

$$\gamma \frac{\langle \nu_H \rangle^2}{M_P l} \nu^c \nu^c. \tag{3.26}$$

We can see that a heavy Majorana scale scenario implies that the $SU(2)_R$ breaking scale should not be much lower than the $SU(4)$ scale and also γ should not be too small. Another important role of the higher dimensional operators is that after inflation the inflaton X decays into RH neutrinos through them to reheat the Universe. In addition, the subsequent decay of these neutrinos can explain the baryon asymmetry via leptogenesis [39,40]. For the reheating temperature, we estimate [38] (see also [41]):

$$T_{\rm RH} \sim \sqrt{\Gamma_X M_{\rm Pl}} \tag{3.27}$$

where the total decay width of the inflaton is given by

$$\Gamma_X \simeq \frac{1}{16\pi} \left(\frac{M_{\nu^c}}{M} \right)^2 M_X \tag{3.28}$$

with $M_{\nu^c} = \gamma \frac{\langle \nu_H \rangle^2}{M_{\rm Pl}}$ the mass of the RH neutrinos and M_X the mass of the inflaton. The later is calculated from the effective mass matrix at the local minimum and approximately is $M_X = 2M \simeq 2\tilde{\lambda} v^2$. Since $M \simeq 10^{13}$ GeV, the decay condition $M_X > M_{\nu^c}$ it is always satisfied for appropriate choices of the parameters $\langle \nu_H \rangle$ and γ. In Figs. 6, we present solutions in $n_s - T_{\rm RH}$ and $r - T_{\rm RH}$ plane with respect to the various parameters of the model. For the computation of $T_{\rm RH}$ we assume that $\langle \nu_H \rangle = M \simeq \tilde{\lambda} v^2$ and we present the results for $\gamma = 0.1$ (solid), $\gamma = 0.5$ (dashed) and $\gamma = 1$ (dotted). In this range of γ values, we have a Majorana mass, $M_{\nu^c} \sim 10^6 - 10^7$ GeV, which decreases as we decrease the value of γ. In addition, gravitino constraints implies a bound for the reheating temperature with $T_{\rm RH} < 10^6 - 10^9$ GeV and as we observe from the plots there are acceptable solutions in this range of values. More precisely, from plots (a) and (c) we see that for $\xi > 0.97$ and $\gamma > 0.5$ most of the results predict $T_{\rm RH} > 10^9$ GeV. However, it is clear that the consistency with the gravitino constraints strongly improves as we

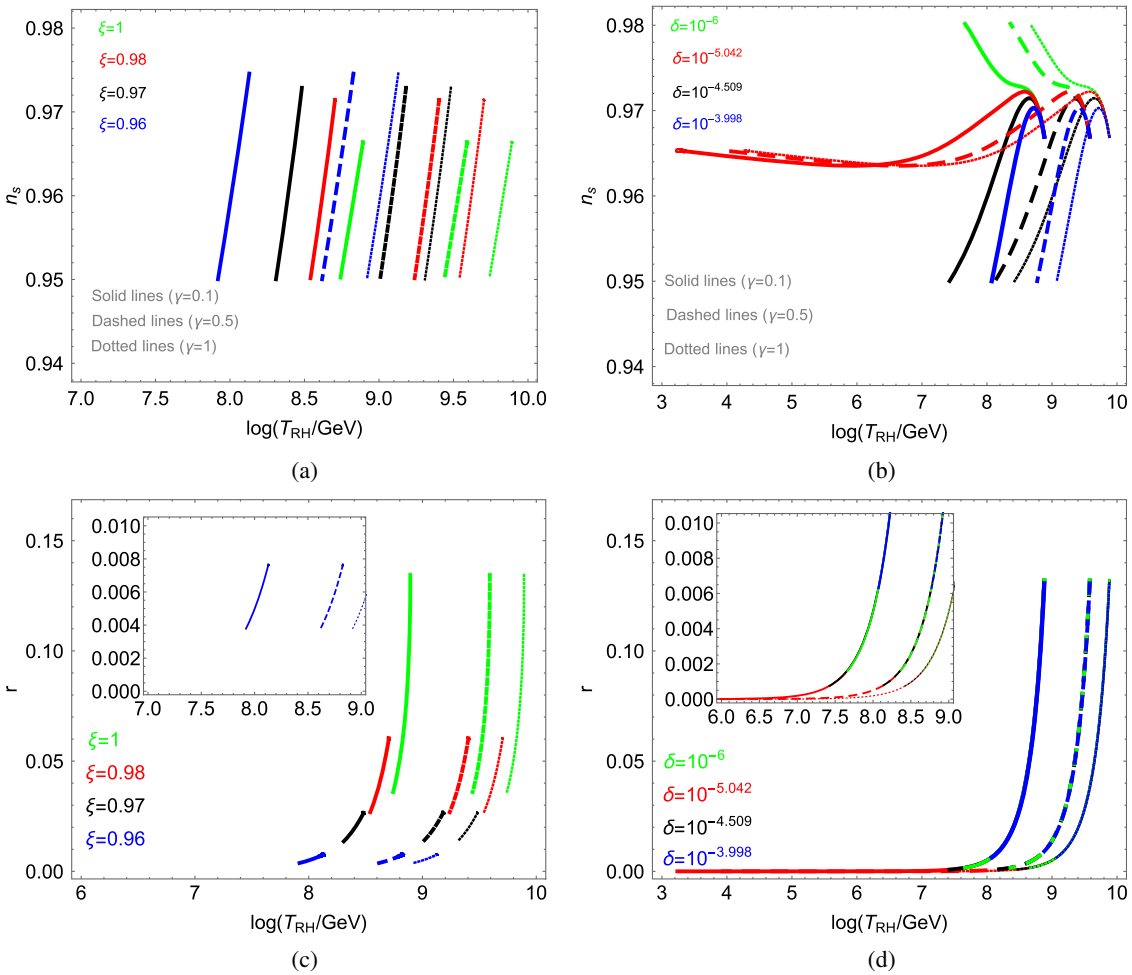

FIG. 6. Plots (a) and (b) show solutions in the $n_s - T_{\rm RH}$ plane by varying the various parameters of the model, while plots (c) and (d) present solutions in the $r - T_{\rm RH}$ plane. In all the cases for the coupling constant γ, we choose the values $\gamma = 0.1$ (solid), $\gamma = 0.5$ (dashed) and $\gamma = 1$ (dotted).

decrease γ, since all the curves with $\gamma = 0.1$ (solid lines) predicts $T_{\rm RH} \lesssim 10^9$ GeV. Similar conclusions can be derived from plots (b) and (d). In addition, from the $r - T_{\rm RH}$ plots (c) and (d) we observe that for $T_{\rm RH} < 10^6 - 10^9$ there are regions in the parameter space with $r \sim 10^{-2} - 10^{-3}$. Furthermore, we observe from plot 6(c) that the tensor-scalar ratio and the reheating temperature are decreased as we decrease the value of ξ since the curves are shift to the left and down regions of the plot.

A sample of the results have been discussed so far is presented in Table I. The table is organized in horizontal blocks and each block contains three sets of values. For each set in a block we change only the coupling constant γ ($\gamma = 1,\ 0.5,\ 0.1$) while we keep $\tilde{\lambda}$, ξ and δ constant. We observe that as we decrease the values of $\tilde{\lambda}$ and ξ the values of the tensor to scalar ratio (r) and the reheating temperature ($T_{\rm RH}$) also decreased.

D. Inflation along S direction

Here we briefly discussed the case where the S field has the rôle of the inflaton. In the potential (3.7), we put $\langle \nu_H \rangle = 0$ and $\langle \bar{\nu}_H \rangle = 0$, so we have

$$V = \frac{144\tilde{\kappa}^2 S^2 (\frac{m}{2\tilde{\kappa}} - S^2)^2}{(3 - S^2)^2}. \tag{3.29}$$

In order to remove the singularity of the denominator, we take $m = 6\tilde{\kappa}$. In this case, we get the following simple form

$$V = 144\tilde{\kappa}^2 S^2 \tag{3.30}$$

which is of the form of a chaotic-potential.

Now the kinetic energy is defined as,

$$\mathcal{L} = \frac{1}{2} K_i^j (\partial S)^2 - 144\tilde{\kappa} S^2 \quad \text{where}$$
$$K_i^j = \frac{\partial^2 K}{\partial S \partial S^*} = \frac{9}{(3 - SS^*)^2}. \tag{3.31}$$

Let $S = \frac{X}{\sqrt{2}}$ then the potential in (3.30) becomes, $V = 72\tilde{\kappa}^2 X^2$, and from the coefficient of the kinetic energy term we can find X in terms of a canonical normalized field χ:

$$X = \sqrt{6} \tanh\left(\frac{\chi}{\sqrt{6}}\right). \tag{3.32}$$

The potential in terms of the canonical normalized field reads as

$$V = 432\tilde{\kappa}^2 \tanh^2\left(\frac{\chi}{\sqrt{6}}\right), \tag{3.33}$$

TABLE I. Inflationary predictions of the model for various values of $\tilde{\lambda}$, ξ, δ and γ. The number of e-folds is taken to be $N = 60$.

$\frac{X_0}{M_{\rm Pl}}$	$\frac{X_e}{M_{\rm Pl}}$	γ	$\tilde{\lambda}$	ξ	δ	$\frac{M_{\rm Inf}}{M_{\rm Pl}}$	$\frac{M_{\nu^c}}{M_{\rm Pl}}$	n_s	r	$\frac{dn_s}{dln\kappa}$	$\log(T_{\rm RH}/{\rm GeV})$
15.04	1.41	1	0.0384	0.9936	10^{-6}	1.16×10^{-5}	3.4×10^{-11}	0.968	0.1070	-4.7×10^{-4}	9.83
15.04	1.41	0.5	0.0384	0.9936	10^{-6}	1.16×10^{-5}	1.7×10^{-11}	0.968	0.1070	-4.7×10^{-4}	9.53
15.04	1.41	0.1	0.0384	0.9936	10^{-6}	1.16×10^{-5}	3.4×10^{-12}	0.968	0.1070	-4.7×10^{-4}	8.84
13.848	1.41	1	0.0304	0.98	$10^{-4.61}$	9.25×10^{-6}	2.139×10^{-11}	0.971	0.057	-2.87×10^{-4}	9.683
13.848	1.41	0.5	0.0304	0.98	$10^{-4.61}$	9.25×10^{-6}	1.07×10^{-11}	0.971	0.057	-2.87×10^{-4}	9.382
13.848	1.41	0.1	0.0304	0.98	$10^{-4.61}$	9.25×10^{-6}	2.139×10^{-12}	0.971	0.057	-2.87×10^{-4}	8.683
12.83	1.40	1	0.02141	0.97	$10^{-4.22}$	6.5×10^{-6}	1.05×10^{-11}	0.967	0.0238	1.5×10^{-6}	9.45
12.83	1.40	0.5	0.02141	0.97	$10^{-4.22}$	6.5×10^{-6}	5.29×10^{-12}	0.967	0.0238	1.5×10^{-6}	9.15
12.83	1.40	0.1	0.02141	0.97	$10^{-4.22}$	6.5×10^{-6}	1.05×10^{-12}	0.967	0.0238	1.5×10^{-6}	8.45
12.69	1.40	1	0.019	0.97	$10^{-3.72}$	5.8×10^{-6}	8.4×10^{-12}	0.958	0.018	2.3×10^{-4}	9.38
12.69	1.40	0.5	0.019	0.97	$10^{-3.72}$	5.8×10^{-6}	4.2×10^{-12}	0.958	0.018	2.3×10^{-4}	9.08
12.69	1.40	0.1	0.019	0.97	$10^{-3.72}$	5.8×10^{-6}	8.4×10^{-13}	0.958	0.018	2.3×10^{-4}	8.3
11.85	1.40	1	0.0118	0.96	$10^{-4.82}$	3.57×10^{-6}	3.2×10^{-12}	0.966	0.0061	5.1×10^{-5}	9.065
11.85	1.40	0.5	0.0118	0.96	$10^{-4.82}$	3.57×10^{-6}	1.6×10^{-12}	0.966	0.0061	5.1×10^{-5}	8.76
11.85	1.40	0.1	0.0118	0.96	$10^{-4.82}$	3.57×10^{-6}	3.2×10^{-13}	0.966	0.0061	5.1×10^{-5}	8.065
11.79	1.40	1	0.010	0.96	$10^{-4.397}$	3.13×10^{-6}	2.5×10^{-12}	0.957	0.0050	2.1×10^{-4}	8.98
11.79	1.40	0.5	0.010	0.96	$10^{-4.397}$	3.13×10^{-6}	1.2×10^{-12}	0.957	0.0050	2.1×10^{-4}	8.67
11.79	1.40	0.1	0.010	0.96	$10^{-4.397}$	3.13×10^{-6}	2.5×10^{-13}	0.957	0.0050	2.1×10^{-4}	7.97
11.64	1.404	1	0.00891	0.958	$10^{-4.5}$	2.71×10^{-6}	1.85×10^{-12}	0.957	0.0034	1.8×10^{-4}	8.89
11.64	1.404	0.5	0.00891	0.958	$10^{-4.5}$	2.71×10^{-6}	9.24×10^{-13}	0.957	0.0034	1.8×10^{-4}	8.59
11.64	1.404	0.1	0.00891	0.958	$10^{-4.5}$	2.71×10^{-6}	1.84×10^{-13}	0.957	0.0034	1.8×10^{-4}	7.89
11.59	1.40	1	0.0084	0.958	$10^{-4.5}$	2.6×10^{-6}	1.64×10^{-12}	0.956	0.00299	1.9×10^{-4}	8.84
11.59	1.40	0.5	0.0084	0.958	$10^{-4.5}$	2.6×10^{-6}	8.2×10^{-13}	0.956	0.00299	1.9×10^{-4}	8.54
11.59	1.40	0.1	0.0084	0.958	$10^{-4.5}$	2.6×10^{-6}	1.64×10^{-13}	0.956	0.00299	1.9×10^{-4}	7.84

which is analogous to the conformal chaotic inflation model or T-Model inflation already mentioned before. Potentials for the T-Model inflation are given in Eq. (3.17). For $n = 1$ the potential become, $V(\chi) = \lambda \tanh^2(\frac{\chi}{\sqrt{6}})$, which is similar to our potential in (3.33) for $\lambda = 432\tilde{\kappa}^2$. We can understand the inflationary behavior in these type of models, by considering two cases.

First for $\chi \geq 1$, by writing the potential in exponential form we have

$$V = \lambda\left(\frac{1-e^{-\sqrt{\frac{2}{3}}\chi}}{1+e^{-\sqrt{\frac{2}{3}}\chi}}\right)^2 = \lambda\left(1-\frac{2e^{-\sqrt{\frac{2}{3}}\chi}}{1+2e^{-\sqrt{\frac{2}{3}}\chi}}\right)^2 = \lambda\left(1-2e^{-\sqrt{\frac{2}{3}}\chi}\right)^2 \tag{3.34}$$

and for large values of χ we can write

$$V \simeq \lambda\left(1-4e^{-\sqrt{\frac{2}{3}}\chi}\right), \tag{3.35}$$

where $\lambda = 432\tilde{\kappa}^2$. The slow roll parameters in terms of the field χ and for large number of e-folds (N) are

$$\frac{d\chi}{dN} = \frac{V'}{V} = 4\sqrt{\frac{2}{3}}e^{-\sqrt{\frac{2}{3}}\chi}. \tag{3.36}$$

Integrating (3.36), we have $\int e^{\chi\sqrt{2/3}}d\chi = \int 4\sqrt{\frac{2}{3}}dN$, which gives the relation

$$e^{-\sqrt{\frac{2}{3}}\chi} = \frac{3}{8N}. \tag{3.37}$$

Using the relation above we have for the slow-roll parameter ϵ that,

$$\epsilon = \frac{1}{2}\left(\frac{V'}{V}\right)^2 = \frac{1}{2}\left(4\sqrt{\frac{2}{3}}e^{-\sqrt{\frac{2}{3}}\chi}\right)^2 = \frac{3}{4N^2}. \tag{3.38}$$

Similarly the second slow-roll parameter η is found to be,

$$\eta = \left(\frac{V''}{V}\right) = -\frac{1}{N}. \tag{3.39}$$

Finally, the predictions for the tensor-to-scalar ratio r and the natural-spectral index n_s are,

$$r = \frac{12}{N^2}, \qquad n_s = 1 + 2\eta - 6\epsilon = 1 - \frac{2}{N} - \frac{9}{4N^2} \tag{3.40}$$

and for $N = 60$ e-foldings we get $n_s \simeq 0.9673$ and $r \simeq 0.0032$.

Regarding the case with $\chi \ll 1$, we can see from the expression (3.33) that the potential reduces to a quadratic chaotic form. The tree-level inflationary predictions in this case are $(n_s, r) \approx (0.967, 0.130)$, which are ruled out with the latest *Planck* 2015 results.

The discussion above strongly depends on the assumption $m = 6\tilde{\kappa}$ that we imposed on the potential in order to simplify it. If we consider small variations of this assumption similar to (3.11) and modify the condition as, $m = 6\tilde{\kappa} + \delta$, we will see that the parameter δ contributes only to n_S while the tensor-to-scalar ratio r remains constant.

IV. CONCLUSIONS

In the present work, we have studied ways to realize the inflationary scenario in a no-scale supersymmetric model based on the Pati-Salam gauge group $SU(4) \times SU(2)_L \times SU(2)_R$, supplemented with a Z_2 discrete symmetry. The spontaneous breaking of the group factor $SU(4) \to SU(3) \times U(1)_{B-L}$ is realized via the $SU(4)$ adjoint $\Sigma = (15, 1, 1)$ and the breaking of the $SU(2)_R$ symmetry is achieved by nonzero vevs of the neutral components $\nu_H, \bar{\nu}_H$ of the Higgs fields $(4, 1, 2)_H$ and $(\bar{4}, 1, 2)_{\bar{H}}$.

We have considered a no-scale structure Kähler potential and assumed that the inflaton field is a combination of ν_H, $\bar{\nu}_H$ and find that the resulting potential is similar with the one presented in [29,30] but our parameter space differs substantially. Consequently, there are qualitatively different solutions which are presented and analyzed in the present work. The results strongly depend on the parameter ξ and for various characteristic values of the latter we obtain different types of inflation models. In particular, for $\xi = 0$ and canonical normalized field $\chi \geq 1$, the potential reduces to Starobinsky model and for $\xi = 1$ the model receives a chaotic inflation profile. The results for $0 < \xi < 1$ have been analyzed in detail while reheating via the decay of the inflaton in right-handed neutrinos is discussed.

We also briefly discussed the alternative possibility where the S field has the rôle of the inflaton. In this case, the potential is exponentially flat for $\chi \geq 1$. Similar conclusions can be drawn for the Starobinsky model. On the other hand, for small χ, it reduces to a quadratic potential.

In conclusion, the $SU(4) \times SU(2)_L \times SU(2)_R$ model described in this paper can provide inflationary predictions consistent with the observations. Performing a detailed analysis, we have shown that consistent solutions with the Planck data are found for a wide range of the parameter space of the model. In addition, the inflaton can provide masses to the right-handed neutrinos and depending on the value of reheating temperature and the right-handed neutrino mass spectrum thermal or nonthermal leptogenesis is a natural outcome. Finally, we mention that, in several cases the tensor-to-scalar ratio r, a canonical measure of primordial gravity waves, is close to $\sim 10^{-2}$–10^{-3} and can be tested in future experiments.

ACKNOWLEDGMENTS

The authors are thankful to George K. Leontaris, Qaisar Shafi, Tianjun Li and Mansoor Ur Rehman for helpful

discussions and useful comments. W. A. would like to thank the Physics Department at University of Ioannina for hospitality and for providing a conducive atmosphere for research where part of this work has been carried out. W. A. was supported by the CAS-TWAS Presidents Fellowship Programme.

[1] A. H. Guth, Phys. Rev. D **23**, 347 (1981).
[2] A. D. Linde, Phys. Lett. **108B**, 389 (1982).
[3] V. F. Mukhanov and G. V. Chibisov, Pis'ma Zh. Eksp. Teor. Fiz. **33**, 549 (1981) [JETP Lett. **33**, 532 (1981)].
[4] A. Albrecht and P. J. Steinhardt, Phys. Rev. Lett. **48**, 1220 (1982).
[5] F. L. Bezrukov and M. Shaposhnikov, Phys. Lett. B **659**, 703 (2008).
[6] E. Cremmer, S. Ferrara, C. Kounnas, and D. V. Nanopoulos, Phys. Lett. **133B**, 61 (1983); J. R. Ellis, A. B. Lahanas, D. V. Nanopoulos, and K. Tamvakis, Phys. Lett. **134B**, 429 (1984).
[7] A. B. Lahanas and D. V. Nanopoulos, Phys. Rep. **145**, 1 (1987).
[8] J. Ellis, D. V. Nanopoulos, and K. A. Olive, Phys. Rev. Lett. **111**, 111301 (2013); **111**, 129902(E) (2013).
[9] D. Roest, M. Scalisi, and I. Zavala, J. Cosmol. Astropart. Phys. 11 (2013) 007.
[10] C. Pallis, J. Cosmol. Astropart. Phys. 04 (2014) 024; 07 (2017) 01(E).
[11] J. Ellis, M. A. G. Garcia, D. V. Nanopoulos, and K. A. Olive, J. Cosmol. Astropart. Phys. 08 (2014) 044.
[12] A. B. Lahanas and K. Tamvakis, Phys. Rev. D **91**, 085001 (2015).
[13] L. Wu, S. Hu, and T. Li, Eur. Phys. J. C **77**, 168 (2017).
[14] M. C. Romao and S. F. King, J. High Energy Phys. 07 (2017) 033.
[15] L. Covi, M. Gomez-Reino, C. Gross, J. Louis, G. A. Palma, and C. A. Scrucca, J. High Energy Phys. 08 (2008) 055; A. Hetz and G. A. Palma, Phys. Rev. Lett. **117**, 101301 (2016).
[16] S. Hardeman, J. M. Oberreuter, G. A. Palma, K. Schalm, and T. van der Aalst, J. High Energy Phys. 04 (2011) 009.
[17] J. C. Pati and A. Salam, Phys. Rev. D **10**, 275 (1974); **11**, 703(E) (1975).
[18] J. C. Pati, Int. J. Mod. Phys. A **32**, 1741013 (2017).
[19] I. Antoniadis and G. K. Leontaris, Phys. Lett. B **216**, 333 (1989).
[20] M. Cvetic, T. Li, and T. Liu, Nucl. Phys. **B698**, 163 (2004).
[21] P. Anastasopoulos, G. K. Leontaris, and N. D. Vlachos, J. High Energy Phys. 05 (**2010**) 011.
[22] M. Cvetic, D. Klevers, D. K. M. PeÃśa, P. K. Oehlmann, and J. Reuter, J. High Energy Phys. 08 (2015) 087.
[23] R. Jeannerot, S. Khalil, G. Lazarides, and Q. Shafi, J. High Energy Phys. 10 (2000) 012.
[24] C. Pallis and N. Toumbas, J. Cosmol. Astropart. Phys. 12 (2011) 002; C. Pallis and N. Toumbas, J. Cosmol. Astropart. Phys. 12 (2011) 002.
[25] B. C. Bryant and S. Raby, Phys. Rev. D **93**, 095003 (2016).
[26] J. Chakrabortty, R. Maji, S. Mohanty, S. K. Patra, and T. Srivastava, Phys. Rev. D **97**, 095010 (2018).
[27] I. Garg and S. Mohanty, Phys. Lett. B **751**, 7 (2015).
[28] S. F. King and Q. Shafi, Phys. Lett. B **422**, 135 (1998).
[29] J. Ellis, H. J. He, and Z. Z. Xianyu, Phys. Rev. D **91**, 021302 (2015).
[30] J. Ellis, H. J. He, and Z. Z. Xianyu, J. Cosmol. Astropart. Phys. 08 (2016) 068.
[31] M. Cicoli, S. de Alwis, and A. Westphal, J. High Energy Phys. 10 (2013) 199.
[32] J. Ellis, D. V. Nanopoulos, and K. A. Olive, J. Cosmol. Astropart. Phys. 10 (2013) 009.
[33] R. Kallosh and A. Linde, J. Cosmol. Astropart. Phys. 06 (2013) 028; 07 (2013) 002.
[34] A. A. Starobinsky, Phys. Lett. **91B**, 99 (1980).
[35] P. A. R. Ade *et al.* (Planck Collaboration), Astron. Astrophys. **594**, A20 (2016).
[36] A. De Simone, M. P. Hertzberg, and F. Wilczek, Phys. Lett. B **678**, 1 (2009).
[37] N. Okada, M. U. Rehman, and Q. Shafi, Phys. Rev. D **82**, 043502 (2010).
[38] G. K. Leontaris, N. Okada, and Q. Shafi, Phys. Lett. B **765**, 256 (2017).
[39] M. Fukugita and T. Yanagida, Phys. Lett. B **174**, 45 (1986).
[40] G. Lazarides and Q. Shafi, Phys. Lett. B **258**, 305 (1991); G. R. Dvali, G. Lazarides, and Q. Shafi, Phys. Lett. B **424**, 259 (1998).
[41] G. Lazarides, Lect. Notes Phys. **592**, 351 (2002).